



SUBJECT AREAS:

MOLECULAR
ELECTRONICS

ELECTRONIC DEVICES

LASERS, LEDS AND LIGHT
SOURCESELECTRONIC PROPERTIES AND
MATERIALS

Received

11 September 2012

Accepted

3 December 2012

Published

17 December 2012

Correspondence and
requests for materials
should be addressed to
S.Z.B. (s.z.bisri@rug.
nl) or T.T. (takenobu@
waseda.jp)

* Current address:

Zernike Institute for
Advanced Materials,
University of
Groningen,
Nijenborgh 4,
Groningen 9747AG
(The Netherlands)

Organic Single-Crystal Light-Emitting Transistor Coupling with Optical Feedback Resonators

Satria Zulkarnaen Bisri^{1*}, Kosuke Sawabe¹, Masaki Imakawa², Kenichi Maruyama², Takeshi Yamao³, Shu Hotta³, Yoshihiro Iwasa^{4,5,6} & Taishi Takenobu²

¹Department of Physics, Graduate School of Science, Tohoku University, 6-3 Aramaki, Aza-Aoba, Aoba-ku, Sendai 980-8578 (Japan), ²Department of Applied Physics, Waseda University, Shinjuku-ku, Tokyo 169-8555 (Japan), ³Department of Macromolecular Science and Engineering, Kyoto Institute of Technology, Matsugasaki, Kyoto 606-8585 (Japan), ⁴Quantum-Phase Electronic Center and Department of Applied Physics, The University of Tokyo, 7-3-1 Hongo, Bunkyo-ku, Tokyo 113-8656 (Japan), ⁵Correlated Electron Research Group (CERG), RIKEN-Advanced Science Institute, Wako, Saitama 351-0198 (Japan), ⁶CREST, Japan Science and Technology Agency (JST), Saitama 332-0012 (Japan).

Organic light-emitting transistors (OLETs) are of great research interest because they combine the advantage of the active channel of a transistor that can control the luminescence of an in-situ light-emitting diode in the same device. Here we report a novel single-crystal OLET (SCLET) that is coupled with single crystal optical feedback resonators. The combination of single-crystal waveguides with native Fabry-Perot cavities, formed by parallel crystal edges, drastically lowers the threshold energy for spectral narrowing and non-linear intensity enhancement. We apply this structure to SCLETs and demonstrate the first fabrication of a SCLET with the optical feedback resonators.

Organic-semiconductor-based devices such as light-emitting diodes (OLEDs), solar cells, memories and field-effect transistors (OFETs) have been predicted to enable low-cost plastic electronics^{1–3}. Recently developed organic light-emitting transistors (OLETs) are a novel class of optoelectronic devices that combine the electrical switching functionality of an OFET and the capability of light generation of an OLED in a single structure^{4–11}. Because of this multifunctional capability, OLETs have potential for use in displays, in integrated optoelectronic components in optical communications, and in sensors apparatuses. Therefore, several studies have examined OLETs fabricated with solution-processed conjugated polymers, vacuum-deposited thin films of small molecules, and single crystals. Thus, the operational performance of OLETs has rapidly improved^{4–17}.

The advantages of organic single crystals, such as high thermal stability, a highly ordered structure, and high carrier mobility (typically greater than $0.1 \text{ cm}^2 \text{ V}^{-1} \text{ s}^{-1}$), made them become attractive candidates for the active materials for radiant optoelectronic devices based on OLETs^{12–17}. The long-range order and the high chemical purity of organic single crystals provide intrinsically excellent charge-carrier transport properties. The mobility value in selected organic single crystals can be three orders of magnitude higher or more than the value in their amorphous phase, without any serious decrease in the luminescence efficiency of the materials^{14,15}. Although these high carrier mobility and luminescence efficiency values are suitable for the future applications of the device, a combination with optical feedback resonators is strongly required for colour tuning and efficient light emission^{18,19}.

It has been relatively easy to introduce cavities in thin-film devices, and many approaches have already been reported^{18,19}. However, fabrication of built-in optical feedback resonators using a single-crystal device is still difficult. Within this framework, several efforts have been made to construct a resonator for organic single crystals. Among of the examples were the use of a naturally-formed cleaved facet as a Fabry-Perot resonator^{20–22}, microcavities fabricated using electron-beam lithography (EBL) and reactive ion etching (RIE)^{23–25}, as well as distributed-feedback cavities prepared using laser ablation method²⁶. As grown single crystals containing natural Fabry-Perot resonator were typically very small in size, and SCLETs fabrication using these crystals was difficult. However, the single crystal processing by EBL, RIE, or laser ablation can physically damage the crystal morphology, thus diminishing the high electronic transport and optical performance (the advantages of single-crystal devices). To the best of our knowledge, the creation of an SCLET exhibiting an optical-cavity effect has



never been reported, although it was possible to introduce the above-mentioned cavities into organic single crystals.

In this study, we present SCLETs that is coupled with a conceptually-novel optical-feedback resonator. The key components of the improved SCLETs are the single-crystal optical waveguide, coupler, and resonator. Optical waveguides and cavities from as-grown organic single crystals are fabricated. A native Fabry-Perot cavity formed by parallel crystal edges is selected as resonator. In addition, effective optical directional coupling between single-crystal waveguides and optical feedback resonator is constructed using a simple crystal-lamination technique. The combination of these optical devices drastically reduces the threshold energy (E_{Th}) for spectral narrowing and nonlinear intensity enhancement of the luminescence in this organic-single-crystal system. To demonstrate the potential of this device architecture, we report the first fabrication of SCLETs with optical-feedback resonators.

Results

Design principles of the SCLET with optical feedback resonators.

Our strategy to overcome the problem in most of the devices with optical resonator is the separation of the light-emitting sub-device and the feedback cavities. **Figure 1a** illustrates our implementation of this concept in which both the light-emitting component and the optical feedback resonator are separately fabricated, but optically coupled. The emitted light from the device propagates along the waveguide and transfers to the resonator by optical coupling. After some time, the light accumulated in the cavity returns to the emitting device. This property is the central concept to be utilized to improve SCLETs using coupling of single-crystal devices and optical feedback resonators. Therefore, to develop a coupling method is the key technique required for this strategy.

One possible solution to fabricate optical-coupling structure is the simple crystal lamination method^{27–29}. The recent development of single-crystal organic transistors provided a deeper understanding of the physics of organic semiconductor, without the influence of grain boundaries, and enabled the realization of very high carrier mobilities ($\sim 40 \text{ cm}^2 \text{ V}^{-1} \text{ s}^{-1}$)³⁰. The key structural feature of these transistors is the molecularly flat single-crystal surface that is free of dangling bonds. This surface facilitates ideal insulator-semiconductor^{27–30}, metal-semiconductor³¹, and semiconductor-semiconductor interfaces³². We utilized this technique to achieve optical coupling between single-crystal devices and feedback resonators.

As the first step toward the fabrication of this proposed novel device, an optical simulation was performed to explore whether the optical coupler can be constructed using two laminated single crystals. **Figure 1b** shows the calculated magnetic field intensity of the propagating light inside the model structure. We simulated an infinite-length single crystal laminated on top of another infinite-length crystal, assuming a 3 nm interlayer space between them. This interlayer corresponds to the steps on the surface of the single crystals, the formation of which is inevitable even on a molecularly flat single-crystal surface. For direct comparison with SCLET, we adopted a PMMA/SiO₂/Si substrate for this simulation (see Method). In the simulation, monochromatic light ($\lambda = 576 \text{ nm}$) was injected into the bottom crystal; and as clearly shown in **Fig. 1b**, the light travelled back and forth between the two crystals. This result strongly suggests that fabrication of an optical coupler using two crystals is possible.

Furthermore, we simulated a more realistic model. As shown in **Fig. 1c**, we replaced one of the crystals with a single crystal with parallel crystal edges, the one expected to facilitate the formation of a native Fabry-Perot cavity. The obtained simulation result showed the beating of the propagating light with a higher intensity than that in **Fig. 1b**. These simulations infer that the coupling between SCLETs and the Fabry-Perot cavities results in a stronger

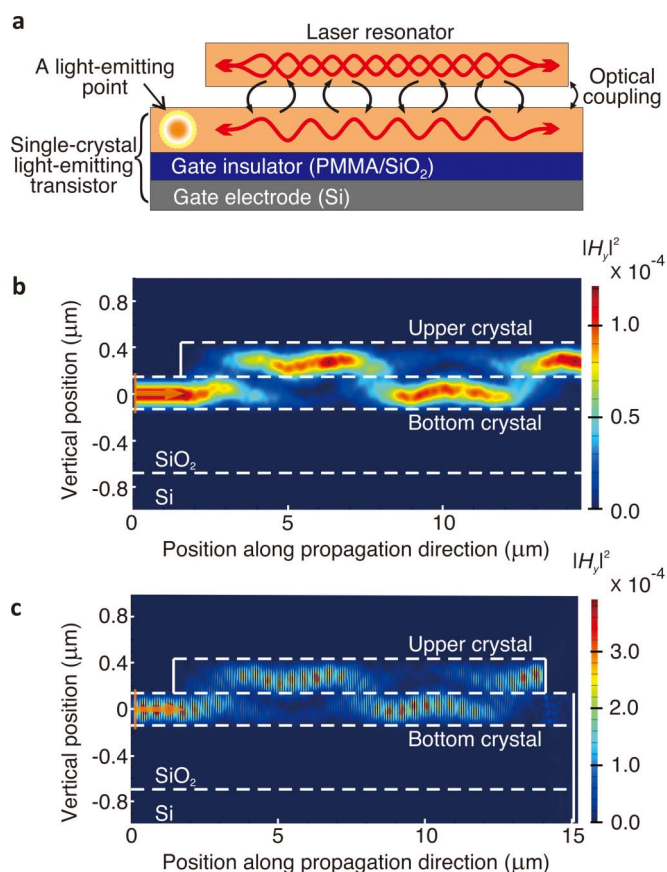


Figure 1 | Design principle of the organic single-crystal device with optical feedback resonators. (a) Conceptual representation of the optically-coupled organic single-crystal light-emitting transistor with an optical feedback resonator. Red lines depict propagating light inside the single-crystal waveguide and feedback resonator. Black arrows indicate optical coupling between the two components. (b) An optical coupling simulation of the design concept. Magnetic field intensity of propagating light ($\lambda = 576 \text{ nm}$, corresponding to the (0–1) peak) is simulated inside an optical directional coupler, which is constructed by laminating BP3T single crystals on top of each other. In the simulation, the light is injected into the bottom crystal. Once the light reaches the area where another crystal is laminated, the light couples into the upper crystal and subsequently transferred back and forth along the propagation path. (c) A similar magnetic field intensity simulation ($\lambda = 576 \text{ nm}$) is performed by considering an additional effect: the effect of the edge of the upper crystal. In addition to the light transfer into the upper crystal, another beating effect of the edge of upper crystal is expected with a higher maximum intensity.

light intensity. Based on this strategy, we developed waveguides, resonators, and couplers that are applicable to single-crystal devices.

Single-crystal waveguides, resonators, and couplers. We chose single crystals of α,ω -bis(biphenyl)terthiophene (BP3T) as the target material for waveguides, resonators, and couplers³³. Absorbance and photoluminescence spectra of BP3T vapour-deposited film are shown in Supplementary Information S1. The reported internal fluorescence-quantum-efficiency of this material was notably high (up to 80% as a single crystal), and it has been known as lasing medium^{34–37}. We carefully selected the best single crystals for waveguides, resonators, and couplers. One of the key structural features for optical waveguides is a defect-free surface. The surface defect can become a scattering centre for light and reduce the quality of waveguide. As shown in **Fig. 2a**, the photoluminescence images of

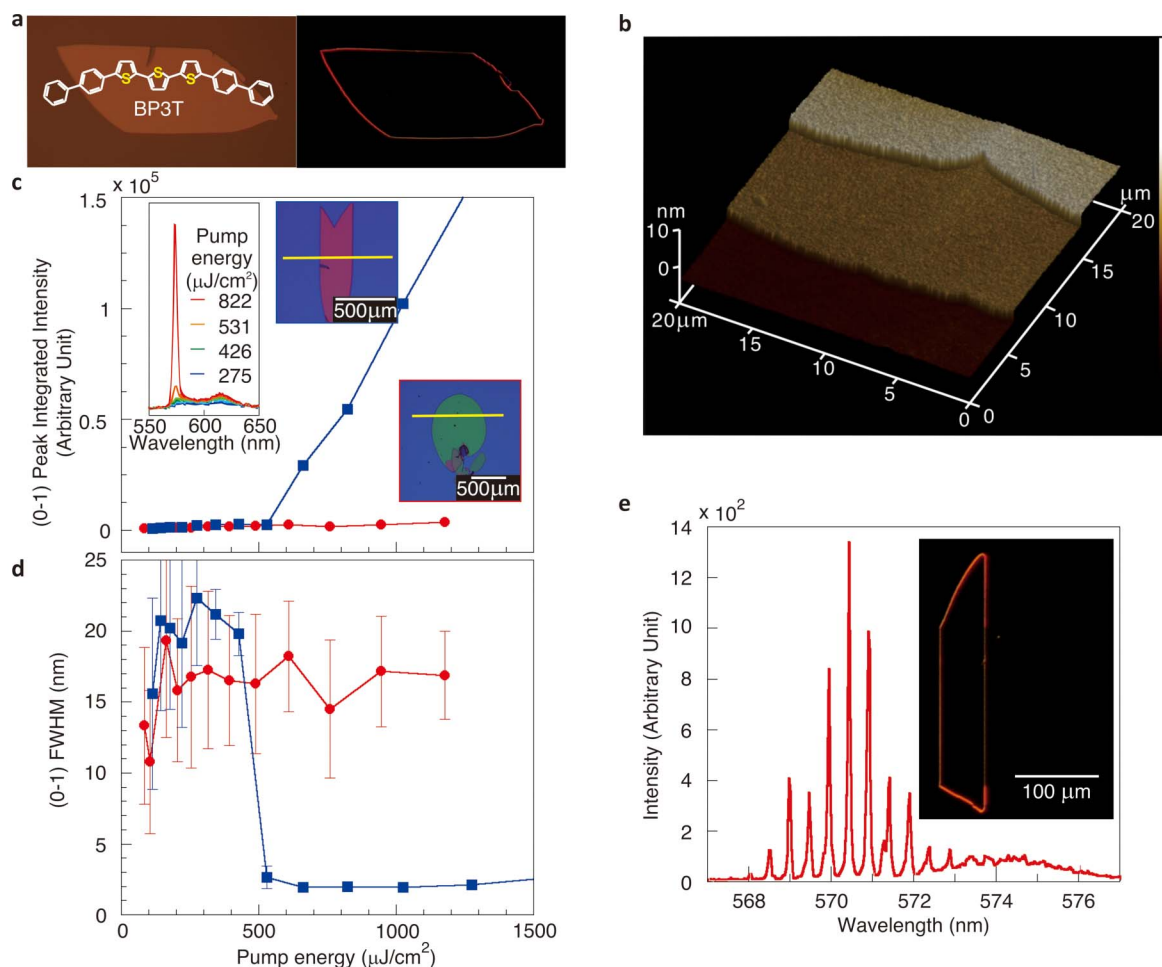


Figure 2 | Organic single-crystal waveguide and resonator. (a) Molecular structure and optical micrograph of α,ω -bis(biphenyl)terthiophene (BP3T) under white (left) and ultraviolet (right) light exposure. (b) A single BP3T crystal imaged by atomic force microscopy. The image shows clear terraces in the BP3T molecular layers. The step height agrees with the c -axis height of the crystal unit cell. (c) Comparison of the integrated intensity of the (0-1) ($\lambda = 576$ nm) peak between a BP3T single crystal with rounded edges (red circle) and a BP3T single crystal with parallel edges (blue square) as a function of the pump laser fluence. The insets show the photoluminescence spectrum of the BP3T crystal with parallel edges as a function of the pump laser fluence (upper right) and optical micrographs of the corresponding crystals (a parallel-edge crystal (upper middle) and a round-edge crystal (bottom right)). The yellow lines indicate the excitation beam. (d) Comparison of the laser-fluence-dependent (0-1) spectral linewidth (full width at half maximum, FWHM) of the respective BP3T crystals. (e) Laser oscillation spectra of the BP3T crystal due to the natural Fabry-Perot resonator of parallel crystal edges. The inset shows an optical micrograph of a corresponding BP3T crystal under ultraviolet light.

single crystals were checked, and the crack-free crystals were collected for the improved SCLETs.

Another key requirement is a molecularly flat single-crystal surface that is free of dangling bonds. This flatness leads to a highly reflective surface, which is a key factor for waveguide quality. The surfaces of the crystals utilized in this study were verified to be molecularly flat by atomic force microscopy (Figure 2b), thereby enabled the usage of a simple lamination technique to construct an optical coupler from two BP3T crystals. The step height on the surface of the BP3T single crystal was approximately 3 nm, corresponded to the half-lattice molecular step¹⁴. This value was also utilized for the optical simulation model. This molecular step will act as the gap between the two crystals.

The remaining component of the device is the single-crystal optical feedback resonator. For this component, we focused our attention on a native Fabry-Perot cavity created by single BP3T crystals. Ichikawa *et al.* reported the laser-oscillation photoluminescence spectrum of crystalline BP3T²⁰. Importantly, this crystal had two naturally-formed parallel facets that acted as a Fabry-Perot optical resonator. To investigate the relationship between crystal shape and the optical cavity effect in this type of single crystal, we

carefully examined the relationship between E_{Th} and crystal shape. To identify the E_{Th} of BP3T single crystals, the emission spectrum was measured as a function of the pump laser fluence (see Methods and Supplementary Information S2). We excited the single crystals with a line-shape-band laser beam measuring approximately 2 mm in length. Figures 2c and 2d illustrate that a single crystal with parallel edges exhibited a clear threshold in both the integrated peak intensity and the full width at half maximum (FWHM). However, threshold behaviour in crystals without Fabry-Perot cavity were not observed in the power range of our excitation laser ($\lambda = 481$ nm). It is clear that the E_{Th} value strongly depends on the shape of the single crystal edge, suggesting that the resonator effect was caused by a native Fabry-Perot cavity.

It should be noted that the broad linewidth of BP3T single crystals (> 20 nm) spectra in Figs. 2c and 2d was also previously observed and reported^{20,34–37}. Despite the observed anomalous broad spectra, a recent time-resolved photoluminescence measurements obviously reported a shortening of the lifetime in both (0-1) ($\lambda = 576$ nm) and (0-2) ($\lambda = 616$ nm) transitions^{36,37}. The reported loss constant in BP3T crystals was $0.074 \text{ dB } \mu\text{m}^{-1}$ ³⁴. To confirm the cavity effect in our BP3T single crystals, as shown in Fig. 2e, we selected a very

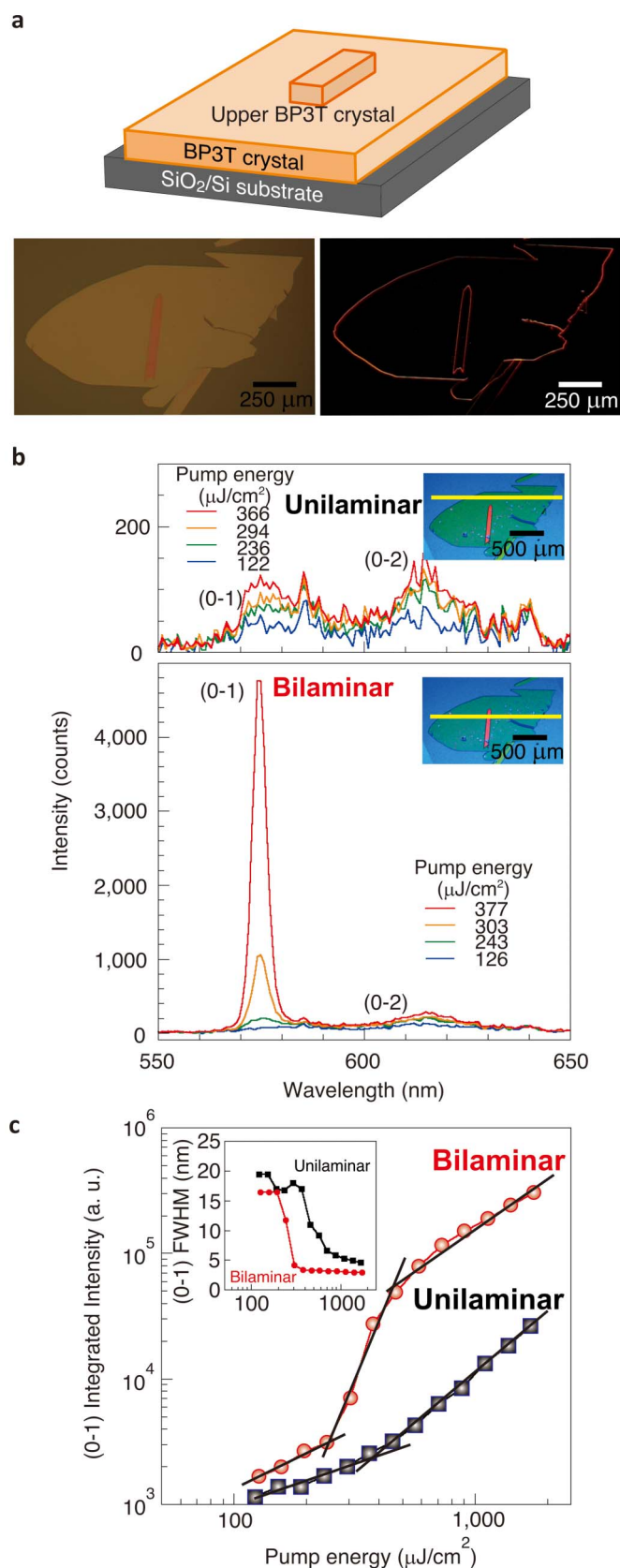


Figure 3 | Organic single-crystal optical coupler. (a) A schematic diagram and optical micrographs of the organic single-crystal optical coupler composed of a small BP3T crystal with parallel edges laminated on top of a larger BP3T crystal to form a bilaminar crystal arrangement. (b) The photoluminescence spectrum of the optical coupler as a function of pump laser fluence. Both the unilaminar (top) and bilaminar crystals (bottom)

were excited. (Insets) Pictures of the organic single crystals contain the yellow lines indicating the excitation position. (c) Comparison of the laser-fluence-dependent integrated intensities of the (0-1) ($\lambda = 576$ nm) peaks between the unilaminar (black square) and bilaminar (red circle) regions.

narrow single crystal ($width = 61 \mu m$) with sharp and parallel crystal edges, then recorded its high-resolution photoluminescence spectrum. We obtained the laser oscillation spectra due to the Fabry-Perot resonator (Fig. 2e) and selected this kind of crystals for the single-crystal optical feedback resonator.

BP3T single crystal with optical feedback resonator. We fabricated the BP3T single crystal with an optical feedback resonator using single crystal waveguides and Fabry-Perot cavities. Figure 3a illustrates the concept behind this new type optical device. The flat crystals without cracks were selected to ensure waveguide quality. It was very difficult to practically fabricate SCLETs using a narrow and small BP3T single crystal. For this reason, we developed a novel optical device by combining a large crystal, which is suitable for transistor fabrications, with a promising crystal feedback resonator. In particular, the optical coupling between the two crystals is the crucial point for this device structure. We laminated a narrow BP3T crystal with a pair of parallel crystal edges that provided excellent qualities as a Fabry-Perot resonator, as shown in Fig. 2e, onto the surface of a larger BP3T crystal. Subsequently, this optical device was examined using laser excitation experiments. We applied a line-shaped band of laser illumination to both the unilaminar and bilaminar configurations (insets of Fig. 3b) to investigate the influence of optical coupling. Interestingly, we observed a clear difference in photoluminescence between the two excitation positions. As shown in Fig. 3b, we excited both unilaminar and bilaminar position with similar energy density up to approximately $370 \mu J cm^{-2}$. At the bilaminar position, the single crystal exhibited a clear threshold in both the integrated peak intensity and the full width at half maximum (FWHM) of the peak. However, at the unilaminar position, we did not observe threshold behaviour in the similar power range. A clear dependence on crystal position was observed for the bilaminar crystal system, suggesting that optical coupling between the two crystals and the resonator effect is caused by the upper cavity crystal. In addition, as shown in Fig. 3c, the bilaminar position exhibited greater slope efficiency than the unilaminar position, as determined by the gradient of the superlinear regime. Although the single-crystal optical device with the small parallel-edge single crystal exhibited enhancement, it was remained unclear whether the two crystals were optically coupled.

To better understand this phenomenon, the size of the irradiating beam (to approximately $200 \mu m$ in length) was decreased and we investigated the position-dependence laser excitation in detail (Fig. 4a and Experimental Section). We scanned the beam position from one edge of the lower crystal to the other edge at a fixed laser power (approximately $1564 \mu J cm^{-2}$) and collected the luminescence spectra. All of the spectra obtained at different excitation points were narrow (Fig. 4b), indicating that the threshold was surpassed (Supplementary Information S3). In Fig. 4c, point with a stronger intensity value indicates a place with lower threshold energy value. First, we observed position-dependent strong photoluminescence spectra when we excited the crystals at position A (Fig. 4c), at which the direction of the emitted light was perpendicular to the parallel edges of the upper crystal. By contrast, excitation at position B led to weaker emission, as shown in Fig. 4c, although the bottom crystal was identical with the one of position A. The peak integrated-intensity values of position A were always stronger than those of position B. The clear difference between position A and position B strongly suggests optical coupling between the two crystals and the existence

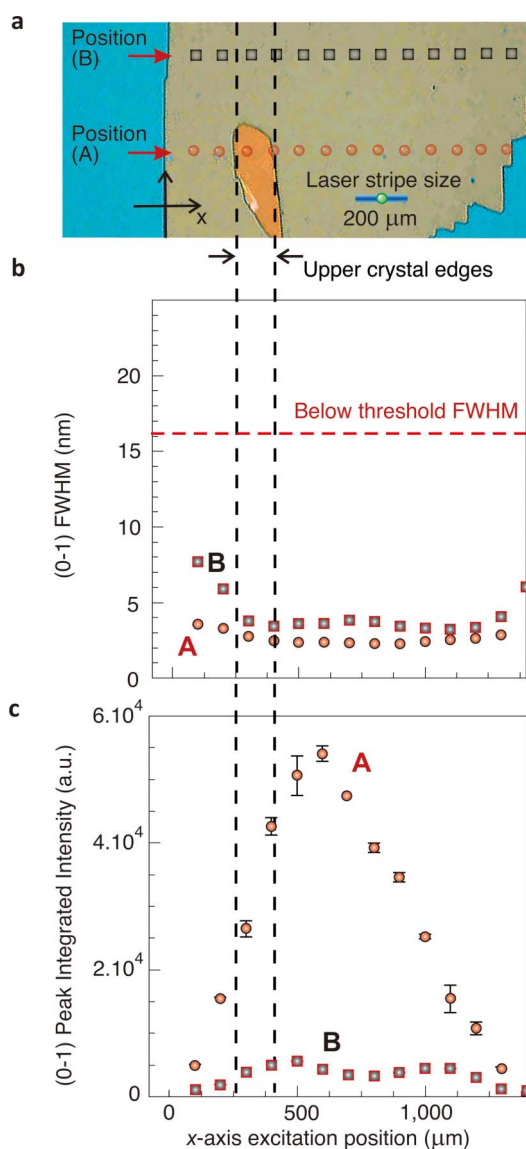


Figure 4 | Position-dependent photo-excitation in bilaminar single-crystal system. (a) Optical micrograph of a bilaminar single crystal and a schematic diagram of the position-dependent spot-excitation measurements using a 200 μm stripe laser beam. The size of the laser stripe is shown on the picture (blue line) with an indicator of the beam centre (green triangle). (b) (0–1) Spectral linewidth (FWHM) during the position-dependent excitation. The red dotted line indicates the normal FWHM. The spectra from both positions A and B are narrow, indicating that all of the position-dependent excitations occurred above the ASE threshold energy. (c) The excitation position-dependent integrated intensity of the (0–1) peak. We excited two different series of crystal positions, labelled as position A and position B. The red arrows indicate the observation directions of the photoluminescence measurements. The red circles and black squares mark the excitation centres of each measurement. Two dashed lines represent the positions of the parallel edges of the upper crystal. Although the measurement path of position A (red circles) crosses the upper crystal, that of position B (black squares) is separated from the upper crystal. The measurements show that the upper crystal leads to a significant enhancement of the emission intensity.

of a second resonator effect caused by the upper Fabry-Perot resonator in position A.

BP3T SCLET with an optical feedback resonator. Finally, the concept of this optical device was applied to the SCLETs (Fig. 5a).

The transistor device fabrication procedures partly have been described in detail elsewhere^{12–16}. Before the metal evaporation step, a small single crystal with a Fabry-Perot cavity was laminated onto an SCLET to create both optical-feedback resonator and optical coupler. Importantly, electrical contact on the upper single crystal (Fig. 5b) was not created to ensure that charge carrier transport only occurred at the interface between the bottom crystal and the dielectric insulator. Clear ambipolar transport was observed (Supplementary Information S4). The ambipolar transport indicates that the utilization of an optical directional coupler do not affect the transport characteristics of the transistor device. Therefore, the recombination process only occurred inside the channel of the bottom crystal.

Figure 5c presents snapshots of the electroluminescence taken from the edge of the SCLET channel during the ambipolar operation. We performed a recombination zone scan along the single crystal channel. The upper image shows the emission when the recombination zone was still near the Ca electrode at which the upper crystal was not connected. At this point, the light only emitted from the bottom crystal. The middle and bottom images show the emission when the recombination zone had already moved toward the area where the upper crystal exists. Interestingly, although there was no direct connection between the Ca electrode and the upper crystal, electroluminescence was also observed from the upper crystal. This result is a further direct evidence of optical coupling between the two single crystals.

Next, we measured the electroluminescence spectra of this edge emission from both the bottom and upper crystals. Figure 5d and 5e show the current-density dependence of the electroluminescence spectra and peak FWHM, respectively. These data were obtained when the device was in ambipolar operation, and the recombination zone positions were in the single-crystal channel where the upper crystal is attached. Initially, when operated at a lower current density, the electroluminescence spectrum behaved as similar as the luminescence spectra of conventional BP3T SCLET. However, at a higher current density, current-driven spectral narrowing with a clear threshold was observed. The occurrence of spectral narrowing with clear threshold behaviour has never been achieved in organic-semiconductor systems that were driven by electric current. Figure 6 shows the current-density dependency of both (0–2) spectral linewidth and the peak intensity obtained from two different devices representing the occurrences of current-driven spectral narrowing. The current-density dependency was compared with the pump-power-dependent spectral narrowing normally achieved in optically-pumped experiment.

Discussion

Before discussing the obtained characteristics from the embedded SCLET device with optical feedback resonator, firstly, the results of the optical measurement on BP3T single crystal that was embedded with optical feedback resonators are examined. At position B, two-peak behaviour of the integrated peak intensity was observed along the x -axis (Fig. 4c). The central dip can be explained by exponential intensity-decay during the light propagation. The emitted light from the excitation position travelled to both sides of the crystal edges, where it was partially reflected by the mirroring crystal facets. Consequently, this feedback light increased the light intensity at the excited area; thus, induced spectral narrowing and non-linear intensity enhancement. This simple consideration leads to the maximum and the minimum intensities occurring at the crystal edges and centre, respectively. Therefore, the observed central valley is well explained by this mechanism. However, the peak behaviours at $x = 500 \mu\text{m}$ and $1000 \mu\text{m}$ cannot be explained by this model. The obtained two-peak behaviour of the integrated intensity at position B (Fig. 4c) strongly indicates an additional optical loss near the bottom-crystal edge. The broader linewidth around both the edges

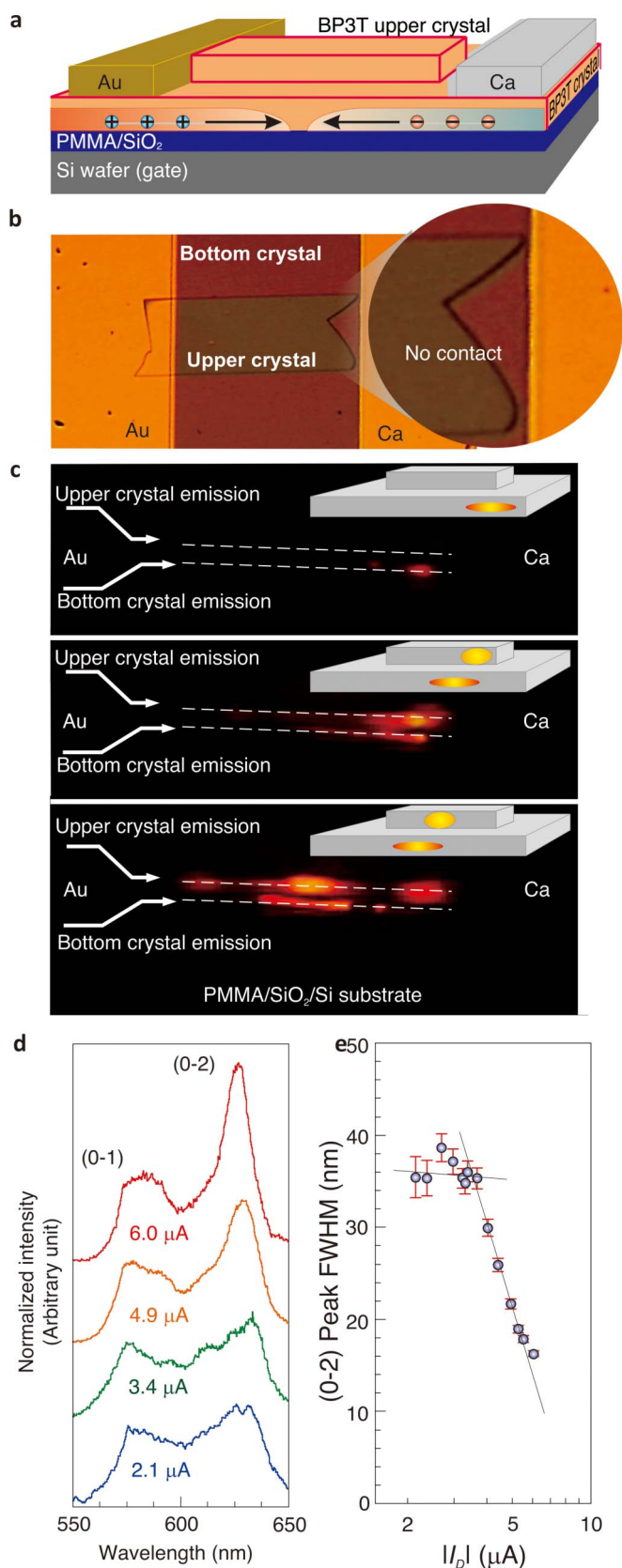


Figure 5 | Organic light-emitting transistor with a single-crystal optical feedback resonator. (a) A schematic of an ambipolar SCLET with a bilaminar BP3T crystal. (b) An optical micrograph of the device channel. Note that there is no electrical contact between the small upper crystal and the Ca electrode. (c) The snapshots of the observed edge emission from the ambipolar SCLET of the bilaminar crystal at different recombination

positions. When the recombination zone is near the Ca electrode (upper image) to which the upper crystal is not connected, the light is only emitted from the bottom crystal. At other places (centre and bottom images), both the top and bottom crystals emit light simultaneously, despite the absence of a direct connection between the Ca electrode and the upper crystal. These indicate optical coupling between the two crystals. The snapshots were taken from the edge of the transistor (see Insets), while the SCLET was operated in ambipolar mode, and the recombination positions were in the single-crystal transistor channel. (d) Current dependence of electro-luminescence spectra from the ambipolar SCLET, exhibiting obvious spectral narrowing of the (0–2) ($\lambda = 616$ nm) peak. (e) Current dependence of the (0–2) peak FWHM; clear threshold behaviour was observed. Note that the device was operated in the ambipolar regime and that its recombination position is in the device channel, which is far from the electrodes.

of the crystal at position B (Fig. 4b) also suggests similar interpretation. If the influence of the upper crystal in position A was not significant, the peak intensity and linewidth behaviours should follow the similar trend as occurred at position B.

The emission intensity values at position A were higher than those at position B, and they were observed without any excitation of the upper Fabry-Perot cavity (Fig. 4c). Even at $x = 1000$ μm , the enhanced intensity was still observed. The spectral linewidths obtained at position A were also always narrower than those at position B, indicating a stronger feedback of light at position A (Fig. 4b).

We can now discuss the cause of the enhancement by the existence of the upper crystal. A simple resonator effect caused by the upper crystal can be immediately excluded, because the enhancement was observed without any excitation of the upper cavity crystal. Moreover, exciton transfer from the bottom to the top crystal can also be completely ruled out based on the result of position-dependence excitation, because the exciton diffusion length of organic materials is much less than 100 μm ^{38,39}. Therefore, the strong improvement in the threshold energy can only be explained by optical coupling between the bottom crystal and the optical resonator (the upper crystal). The light emitted from the bottom crystal transfers to the upper crystal through directional optical coupling and accumulates in the optical resonator (upper crystal). Finally, the resonated light returns to the bottom crystal. The drastic change in the high resolution spectra resulting from the lamination of the upper crystal also supports this interpretation (Supplementary Information S5). The resulting light propagation between the two crystals is known as optical directional coupling^{40,41}.

We now discuss the origin of the single-peak behaviour of the integrated peak intensity at position A as shown in Fig. 4c. To transfer light from the bottom to the upper crystal cavity, the optical path below the upper crystal must be sufficiently long. The lack of a second intensity peak between the upper resonator crystal and the closer bottom crystal edge can be explained by the additional optical loss near the bottom crystal edge. The broader linewidth at $x = 0 - 200$ μm of position A supports this mechanism scenario. The fully understanding of the excitation-position-dependent behaviour is an important issue that remains to be addressed in the future. The main finding of this study itself was the observation of a cavity effect in this bilaminar crystal system. The threshold behaviour for many bilaminar crystal pairs were tested. A minimum threshold energy of as low as 115 $\mu\text{J cm}^{-2}$ was observed for the optically coupled Fabry-Perot resonator pair (see Supplementary information S6) in which both upper and bottom crystals have parallel edges.

Next, the origin of the spectral behaviour of the electroluminescence from the SCLET device is discussed. The increase of the ambipolar current density enhanced the intensity of the (0–2) transition. It should be noted that the narrowing behaviour of the (0–2) transition has also been previously reported^{34–37}. We measured

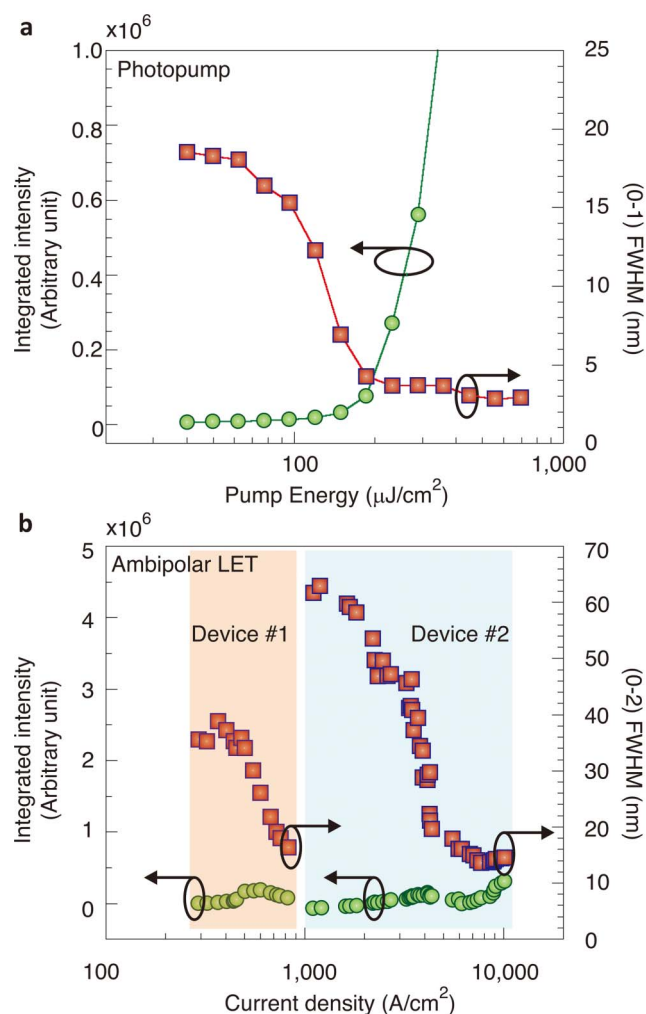


Figure 6 | The photopump laser threshold and the performance of ambipolar SCLET with optical feedback resonator. (a) The plot of the (0–1) peak integrated intensity and FWHM of bilaminar BP3T single crystal with the lowest energy threshold for laser ($E_{th} = 115 \mu\text{J}/\text{cm}^2$) during the photopumped laser measurement. Note that in general, the threshold of the spectral narrowing is lower than the threshold of intensity enhancement. (b) The plot of the current-density dependence of the (0–2) peak integrated intensity and the FWHM from two different bilaminar BP3T ambipolar SCLETs that exhibit spectral narrowing behaviour. The current density is estimated by assuming a 1 nm recombination-zone thickness. There is approximately one order of magnitude difference in the current density threshold of spectral narrowing between device #1 and device #2, indicating strong device dependency.

photoluminescence spectra of several BP3T crystals, and indeed some of them also showed major enhancement of the (0–2) transition (Supplementary Information S7) rather than the (0–1) transition. This finding indicates a strong sample dependency on the photoluminescence spectra of the crystals. The spectral narrowing of the (0–2) transition is allowed for both optical and electrical excitations in BP3T crystals. Although the mechanism of the selection rule remains unclear, these results suggest that the observed enhancement of the (0–2) transition in SCLETs coupling with an optical-feedback resonator is well-explained by the cavity effect of the upper crystal.

From the other viewpoint, the origin of the narrowing behaviour cannot be explained by electric-current-related loss mechanisms, such as those associated with absorption by polarons and triplet excitons, despite the device was operated at very high current density.

Recently, we reported SCLET with patterned unilaminar single crystal, so that the current was confined to produce even higher current density of $33 \text{ kA}/\text{cm}^2$ ¹⁷. However, no spectral narrowing behaviour has been observed from those devices. Therefore, the coupling between the bottom crystal and the upper single crystal consisting native Fabry-Perot cavities of parallel crystal edges is justified to be able to promote a spectral narrowing in SCLETs at high current-density operation. Nevertheless, the effect of current on the other optical properties of the active material, such as refractive index, polarization and optical gain, should be further investigated. To achieve a full understanding of the observed current-driven spectral narrowing is still an important issue that remains to be addressed.

In conclusion, we fabricated a single-crystal optical waveguide, cavity, and coupler. The combination of these optical devices drastically reduced the threshold energy of spectral narrowing and non-linear intensity enhancement, suggesting that a cavity effect was produced in the optical feedback resonator. The application of this technique to SCLETs led to the first fabrication of a SCLET with an optical resonator. The observed clear spectral narrowing behaviour represented evidence for the existence of a cavity effect. These results open a route to the development of colour-tuneable and highly efficient SCLETs as well as electro-optical interconnecting devices.

Methods

Optical simulation. The simulation was performed using Lumerical MODE® (academic license) and Lumerical FDTD® (evaluation license) software. We constructed a model of a bilaminar BP3T single crystal laminated on PMMA (4 nm)/SiO₂ (500 nm)/Si substrate. The thickness of both single crystals was set at 276 nm, which was the average thickness of the grown BP3T. We used the standard wavelength-dependent refractive indices for PMMA, SiO₂ and Si elements. For the BP3T single crystals, we assumed a refractive index value of 4.2 for the *c*-axis direction³⁶. Since the emission of BP3T single crystals was highly polarized in the transverse magnetic (TM) mode¹⁴, only the distribution of the magnetic field was presented in the simulated configurations. A TM mode was thus injected into the single crystal waveguide of the bottom crystal. We used 3 nm for the thickness value of the interlayer spacing by assuming that there would be at least one molecular step on one of the crystal surfaces and a distortion of local refractive index at the interface related with electronic band bending due to molecular strain, charge transfer, or electrostatic force.

Sample fabrication. BP3T crystals were grown using a physical vapour transport method. The complete BP3T crystal growth technique was described elsewhere¹⁴. A large amount of thin BP3T crystal platelets (< 1 000 nm thick) of various shapes and sizes (measuring up to 5 mm in diameter) was obtained.

Optical characterisation. Photopumped ASE measurements were performed by irradiating the BP3T single-crystal samples with a linear pulsed laser beam. The pump pulses were generated by a dye laser (Coumarin 481, Exciton Corp.) that was excited by a nitrogen gas laser (Photonics Technology International Corp GL-3300, $\lambda = 337 \text{ nm}$ with a pulse width of 1 ns). The pump pulses were generated at $\lambda = 481 \text{ nm}$, chosen to match the BP3T absorption band edge, and a pulse width of 800 ps. A neutral density filter was used to adjust the excitation intensities. The laser beam was collimated, expanded to 2 mm in diameter and focused to produce a (theoretical) $2 \text{ mm} \times 30.56 \mu\text{m}$ -wide stripe using a cylindrical lens. The actual beam profile used to estimate the pump energy is explained in Supplementary Information S2. The pump beam was polarized parallel to the long axis of the stripe. Photoluminescence emission was collected from the edges of the crystal samples using a multichannel spectrometer (C-10027, Hamamatsu Photonics, Co.) and an optical fibre. For high resolution spectra measurement, Shamrock SR303i (Andor Technology) high resolution spectrograph was used. A charge-coupled device (CCD) camera with a long-working-distance optical microscope was placed at a 30° angle to the pump beam axis to monitor the positions of the single crystal, the excitation beam, and the photoluminescence emission. The photopumped laser measurements were performed under atmospheric conditions at room temperature. As has been previously reported^{34–37}, there is a competition for laser between the (0–1) and (0–2) peaks of the BP3T spectra (Supplementary Information S7).

Position-dependent measurements. For the position-dependent photopumped measurements, the length of the excitation beam was reduced from 2 mm to 200 μm (measured value, $1/e^2$) by means of a slit before reaching the cylindrical lens. The beam profiling indicated that the broadening effect due to diffraction was limited, thus providing a sufficient number of data points. The slit was placed directly in front of the maxima of the incoming laser beam. The excitation beam position was controlled with a micrometre-precision *x*-*y* translation stage. The centre position of the excitation beam was monitored by the CCD camera with an optical microscope.



SCLET sample fabrication. The single crystals were never exposed to ambient air during the fabrication of the light-emitting transistor^{12–16,42–45}. A large (millimetre-size) BP3T single crystal was mounted onto a PMMA (4–6 nm)/SiO₂ (500 nm)/Si substrate. A small BP3T crystal with parallel edges was subsequently laminated on top of the larger crystal. The lamination of the small crystal was controlled precisely such that the parallel edges were placed in line with the expected channel length direction. The lamination processes of both crystals were performed cautiously to avoid any formation of air bubbles in the expected channel area. Au and Ca were used as the source and drain electrodes, respectively, to optimize hole and electron injection. Importantly, for these ambipolar bilaminar crystal SCLETs, any generation of electrical contact with the upper single crystal was avoided. All device fabrication processes were performed inside a dry N₂ glovebox, including the lamination of the small crystal onto the larger one.

SCLET characterization. The complete SCLET characterization method has been described elsewhere^{12–16,45}. The light-emitting transistors were characterized in the dark inside the glovebox using a semiconductor parameter analyser (Agilent E5270 series) and an optical microscope (Keyence VH-Z100R). Electric pulse measurement was performed with the maximum capability of the semiconductor parameter analyser, which was 500 μ s pulse width with 5 ms pulse period. The microscope was focused to cover both the upper and lower crystal edges. A 3CCD camera (Olympus CS230B) was used for observation, and an ORIEL Fixed Imaging Compact Spectrograph (FICS-model 77440) with a Peltier-cooled detector (Andor DV401A-UVB) was used for spectrum collection. The time-dependent spectral acquisition of the spectrograph was synchronized with the output time of the semiconductor parameter analyser to obtain the current-dependent electroluminescence spectra. The temperature of the device was stabilized at 20°C using a Peltier cooler system mounted on the sample stage.

- Forrest, S. R. The path to ubiquitous and low-cost organic electronic appliances on plastic. *Nature* **428**, 911–918 (2004).
- Dimitrakopoulos, C. D. & Malenfant, P. R. L. Organic Thin Film Transistors for Large Area Electronics. *Adv. Mater.* **14**, 99–117 (2002).
- Gunes, S., Neugebauer, H. & Sariciftci, N. S. Conjugated Polymer-based Organic Solar Cells. *Chem. Rev.* **107**, 1324–1338 (2007).
- Rost, C. *et al.* Light-emitting ambipolar organic heterostructure field-effect transistor. *Synth. Metals* **146**, 237–241 (2004).
- Swensen, J. S., Soci, C. & Heeger, A. J. Light emission from an ambipolar semiconducting polymer field-effect transistor. *Appl. Phys. Lett.* **87**, 253511 (2005).
- Zaumseil, J., Friend, R. H. & Sirringhaus, H. Spatial control of the recombination zone in an ambipolar light-emitting organic transistor. *Nature Mater* **5**, 69–74 (2006).
- Muccini, M. A bright future for organic field-effect transistors. *Nature Mater* **5**, 605–613 (2006).
- Cicoira, F. & Santato, C. Organic Light Emitting Field Effect Transistors: Advances and Perspectives. *Adv. Funct. Mater.* **17**, 3421–3434 (2007).
- Namdas, E. B. *et al.* Gate-Controlled Light Emitting Diodes. *Adv. Mater.* **20**, 1321–1324 (2008).
- Capelli, R. *et al.* Organic light-emitting transistors with an efficiency that outperforms the equivalent light-emitting diodes. *Nature Mater.* **9**, 496–503 (2010).
- Muccini, M., Koopman, W. & Toffanin, S. The photonic perspective of organic light-emitting transistors. *Laser Photonics Rev.* **6**, 258–275 (2011).
- Takahashi, T., Takenobu, T., Takeya, J. & Iwasa, Y. Ambipolar light-emitting transistors of a tetracene single crystal. *Adv. Funct. Mater.* **17**, 1623–1628 (2007).
- Takenobu, T. *et al.* High current density in light-emitting transistors of organic single crystals. *Phys. Rev. Lett.* **100**, 066601 (2008).
- Bisri, S. Z. *et al.* High mobility and luminescent efficiency in organic single-crystal light-emitting transistors. *Adv. Funct. Mater.* **19**, 1728–1735 (2009).
- Yomogida, Y. Y. *et al.* Green light emission from the edges of organic single-crystal transistors. *Appl. Phys. Lett.* **97**, 173301 (2010).
- Bisri, S. Z. *et al.* p-i-n Homostructure in Organic Light-Emitting Transistors. *Adv. Mater.* **23**, 2753–2758 (2011).
- Sawabe, K. *et al.* Current-Confinement Structure and Extremely High Current Density in Organic Light-Emitting Transistors. *Adv. Mater.* **24**, 6141–6146 (2012).
- Samuel, I. D. W. & Turnbull, G. A. Organic semiconductor lasers. *Chem. Rev.* **107**, 1272–1295 (2007).
- Gwinner, M. C. *et al.* Integration of a rib waveguide distributed feedback structure into a light-emitting polymer field-effect transistor. *Adv. Funct. Mater.* **19**, 1360–1370 (2009).
- Ichikawa, M. *et al.* Photopumped laser oscillation and charge-injected luminescence from organic semiconductor single crystals of a thiophene/phenylene co-oligomer. *Appl. Phys. Lett.* **87**, 221113 (2005).
- Ichikawa, M. *et al.* Laser Oscillation in Monolithic Molecular Single Crystals. *Adv. Mater.* **17**, 2073–2077 (2005).
- Yamamoto, T. *et al.* Laser oscillation in a highly anisotropic organic crystal with a refractive index of 4.0. *J. Appl. Phys.* **103**, 093115 (2008).
- Sasaki, F. *et al.* Microdisk and Microring Lasers of Thiophene-Phenylene Co-oligomers Embedded in Si/SiO₂ Substrates. *Adv. Mater.* **19**, 3653–3655 (2007).
- Fujiwara, S. *et al.* Laser oscillations of whispering gallery modes in thiophene/phenylene co-oligomer microrings. *Appl. Phys. Lett.* **91**, 021104 (2007).
- Sasaki, F. *et al.* Microdisk lasers and field effect transistors of thiophene/phenylene co-oligomers by using high temperature deposition method. *Org. Electron.* **11**, 1192–1198 (2010).
- Fang, H.-H. *et al.* Distributed Feedback Lasers Based on Thiophene/Phenylene Co-Oligomer Single Crystals. *Adv. Funct. Mater.* **22**, 33–38 (2012).
- De Boer, R. W. I., Gershenson, M. E., Morpurgo, A. F. & Podzorov, V. Organic single-crystal field-effect transistors. *Phys. Stat. Sol. A* **201**, 1302–1331 (2004).
- Gershenson, M. E., Podzorov, V. & Morpurgo, A. F. Colloquium: Electronic transport in single-crystal organic transistors. *Rev. Mod. Phys.* **78**, 973–989 (2006).
- Hasegawa, T. & Takeya, J. Organic field-effect transistors using single crystals. *Sci. Technol. Adv. Mater.* **10**, 024314 (2009).
- Takeya, J. *et al.* Very high-mobility organic single-crystal transistors with in-crystal conduction channels. *Appl. Phys. Lett.* **90**, 102120 (2007).
- Kaji, T., Takenobu, T., Morpurgo, A. F. & Iwasa, Y. Organic single-crystal schottky gate transistors. *Adv. Mater.* **21**, 3689–3693 (2009).
- Alves, H., Molinari, A. S., Xie, H. X. & Morpurgo, A. F. Metallic conduction at organic charge-transfer interfaces. *Nature Mater.* **7**, 574–580 (2008).
- Hotta, S., Kimura, H., Lee, S. A. & Tamaki, T. Synthesis of thiophene/phenylene co-oligomers. II[1]. block and alternating co-oligomers. *J. Heterocycl. Chem.* **37**, 281–286 (2000).
- Kanazawa, S., Ichikawa, M., Koyama, T. & Taniguchi, Y. Self-waveguided photoemission and lasing of organic crystalline wires obtained by an improved epitaxial growth method. *Chem. Phys. Chem.* **7**, 1881–1884 (2006).
- Hiramatsu, T., Matsuoka, N., Yanagi, H., Sasaki, F. & Hotta, S. Gain-narrowed emissions of thiophene/phenylene co-oligomer single crystals. *Phys. Stat. Sol. (c)* **6**, 338–341 (2009).
- Matsuoka, N. *et al.* Amplified Pulse Emissions with Variable Delay Times in Vibronic Transition Bands of Thiophene/Phenylene Co-Oligomer Single Crystals. *Jpn. J. Appl. Phys.* **49**, 052401 (2010).
- Yanagi, H. *et al.* Prethreshold Lasing with Time-Delayed Pulse Emission from a Single Crystal of Thiophene/Phenylene Co-Oligomer. *Appl. Phys. Express* **4**, 062601 (2011).
- Najafav, H., Lee, B., Zhou, Q., Feldman, L. C. & Podzorov, V. Observation of long-range exciton diffusion in highly ordered organic semiconductors. *Nature Mater.* **9**, 938–943 (2010).
- Mikhnenko, O. V., Ruiter, R., Blom, P. W. M. & Loi, M. A. Direct measurement of the triplet exciton diffusion length in organic semiconductors. *Phys. Rev. Lett.* **108**, 137401 (2012).
- Somekh, S., Garmire, E., Yariv, A., Garvin, H. L. & Hunsperger, R. G. Channel optical waveguide directional couplers. *Appl. Phys. Lett.* **22**, 46 (1973).
- Alfness, R. C. Guided-wave devices for optical communication. *IEEE J. Quantum Elec.* **QE-17**, 946 (1981).
- Takahashi, T., Takenobu, T., Takeya, J. & Iwasa, Y. Ambipolar organic field-effect transistors based on rubrene single crystals. *Appl. Phys. Lett.* **88**, 033511 (2006).
- Takenobu, T., Takahashi, T., Takeya, J. & Iwasa, Y. Effect of metal electrodes on rubrene single-crystal transistors. *Appl. Phys. Lett.* **90**, 013507 (2007).
- Bisri, S. Z. *et al.* Ambipolar field-effect transistor of high photoluminescent material tetraphenylpyrene (TPPy) single crystal. *Jpn. J. Appl. Phys.* **46**, L596–L598 (2007).
- Sawabe, K. *et al.* High current densities in a highly photoluminescent organic single-crystal light-emitting transistor. *Appl. Phys. Lett.* **97**, 043307 (2010).

Acknowledgments

This study was partially supported by JST/PRESTO, JST/CREST, a Grant-in Aid for Scientific Research (Grant No. 22656003), and the Funding Program for Next Generation World-Leading Researchers. S.Z.B. was also supported by the Sasakawa Scientific Research Grant from the Japan Science Society.

Author contributions

S.Z.B., Y.I. and T.T. designed the research and conceived the experiments; S.Z.B., K.S., M.I. and K.M. performed the experiments; S.Z.B. performed the simulations and analyzed data; T.Y. and S.H. supplied the active materials; and S.Z.B. and T.T. wrote the paper.

Additional information

Supplementary information accompanies this paper at <http://www.nature.com/scientificreports>

Competing financial interests: The authors declare no competing financial interests.

License: This work is licensed under a Creative Commons Attribution-NonCommercial-ShareAlike 3.0 Unported License. To view a copy of this license, visit <http://creativecommons.org/licenses/by-nc-sa/3.0/>

How to cite this article: Bisri, S.Z. *et al.* Organic Single-Crystal Light-Emitting Transistor Coupling with Optical Feedback Resonators. *Sci. Rep.* **2**, 985; DOI:10.1038/srep00985 (2012).